DNA Nanotechnology

International Edition: DOI: 10.1002/anie.201910606
German Edition: DOI: 10.1002/ange.201910606

Bottom-Up Assembly of DNA–Silica Nanocomposites into Micrometer-Sized Hollow Spheres

*Yong Hu, Maximilian Grösche, Sahana Sheshachala, Claude Oelschlaeger, Norbert Willenbacher, Kersten S. Rabe, and Christof M. Niemeyer**

Abstract: *Although DNA nanotechnology has developed into a highly innovative and lively field of research at the interface between chemistry, materials science, and biotechnology, there is still a great need for methodological approaches for bridging the size regime of DNA nanostructures with that of micrometer- and millimeter-sized units for practical applications. We report on novel hierarchically structured composite materials from silica nanoparticles and DNA polymers that can be obtained by self-assembly through the clamped hybridization chain reaction. The nanocomposite materials can be assembled into thin layers within microfluidically generated water-in-oil droplets to produce mechanically stabilized hollow spheres with uniform size distributions at high throughput rates. The fact that cells can be encapsulated in these microcontainers suggests that our concept not only contributes to the further development of supramolecular bottom-up manufacturing, but can also be exploited for applications in the life sciences.*

The sequence-specific binding properties of nucleic acids have been exploited over the past 35 years to establish the field of DNA nanotechnology,[1] which has developed into a highly innovative and lively field of research at the interface of chemistry, materials science, biotechnology, and nanotechnology.[2] At present, it is becoming clearly evident that the various sub-disciplines of DNA nanotechnology, ranging from pure "structural DNA nanotechnology"[3] over protein DNA assemblies,[4] nanoparticle-based DNA materials,[5] and DNA polymers[6] to DNA surface technology,[7] are growing ever closer together to create functional devices for applications in the bio- and materials sciences.[2g] However, there is still a great need for methodological approaches to bridge the size regime of individual DNA nanostructures with that of micrometer- and millimeter-sized units for real-world applications.

The self-assembly of materials in microfluidic environments has become an indispensable toolbox technology to demonstrate, control, and understand the fundamentals of these supramolecular processes and to develop advanced processing tools for the manufacturing and integration of components.[8] For example, Spatz and co-workers have recently reported on the assembly of biofunctionalized droplets of water-in-oil emulsions using gold nanoparticles as mechanical stabilizer of the oil/water interface.[9] In the field of DNA nanotechnology, Kurokawa and co-workers recently demonstrated that the stability of batch-produced, cell-sized liposomes and droplets can be enhanced by assembling Y-shaped DNA oligomers on the inner surface of cationic lipid membrane vesicles to form a thin polymeric DNA shell that increases the interfacial tension, elastic modulus, and shear modulus of the droplet surface.[10] Inspired by these approaches and based on earlier investigations of the excellent biomolecular modifiability and biostability of DNA-modified silica nanoparticles (DNA-SiNPs),[11] we wanted to investigate whether the self-assembly of novel composite materials of DNA-SiNPs and DNA polymers at the inner interface of microfluidic droplets is possible. Indeed, we found that polymerization of SiNPs capped with primers for clamped hybridization chain reaction (C-HCR)[12] gives ready access to a novel class of composite materials that display material properties that are distinctively different from those of conventional DNA hydrogels. We demonstrate that the new composites self-assemble underneath the interfacial layer of positively charged water-in-oil (W/O) droplets, thus enabling the high-throughput fabrication of micrometer-sized hollow spheres that could be used for biomedical research.

We initially investigated whether DNA-SiNPs can be converted into polymer composites using the C-HCR. To this end, zwitterion-stabilized SiNPs of 80 nm diameter bearing poly(ethylene glycol) (PEG) chains in addition to amino, phosphonate, and thiol functional groups were synthesized by hydrolysis of silanes in a microemulsion system as previously described (see the Supporting Information, Figure S1),[11c,d] and functionalized with the aminoalkyl-modified 44-mer single-stranded DNA (ssDNA) oligomer **Ih** by glutardialdehyde crosslinking (Figure 1; for DNA sequences, see Table S1 in the Supporting Information). The about 100 **Ih** molecules per **SiNP-Ih** (Table S2) serve as initiators that trigger the self-

[*] M. Sc. Y. Hu, Dr. M. Grösche, M. Sc. S. Sheshachala, Dr. K. S. Rabe, Prof. Dr. C. M. Niemeyer
Karlsruhe Institute of Technology (KIT)
Institute for Biological Interfaces (IBG 1)
Hermann-von-Helmholtz-Platz 1
76344 Eggenstein-Leopoldshafen (Germany)
E-mail: niemeyer@kit.edu
Homepage: https://www.niemeyer-lab.de
Dr. C. Oelschlaeger, Prof. Dr. N. Willenbacher
Karlsruhe Institute of Technology (KIT)
Institute for Mechanical Process Engineering and Mechanics
Gotthard-Franz-Straße 3, 76131 Karlsruhe (Germany)
Supporting information and the ORCID identification number(s) for the author(s) of this article can be found under: https://doi.org/10.1002/anie.201910606.

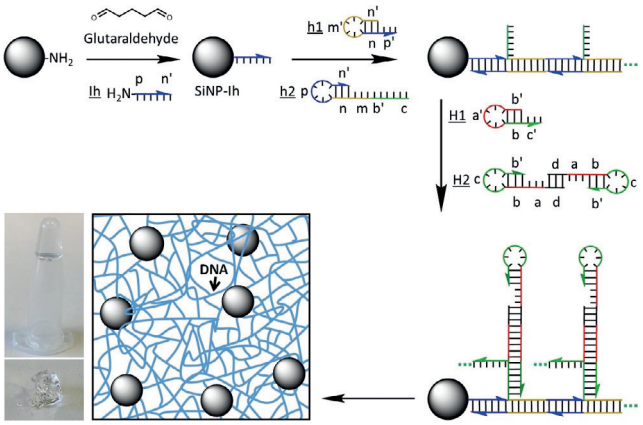

Figure 1. Synthesis of initiator-modified SiNPs and their polymerization by the clamped hybridization chain reaction (C-HCR). The insets are photographic images of the resulting DNA-SiNP nanocomposite hydrogels.

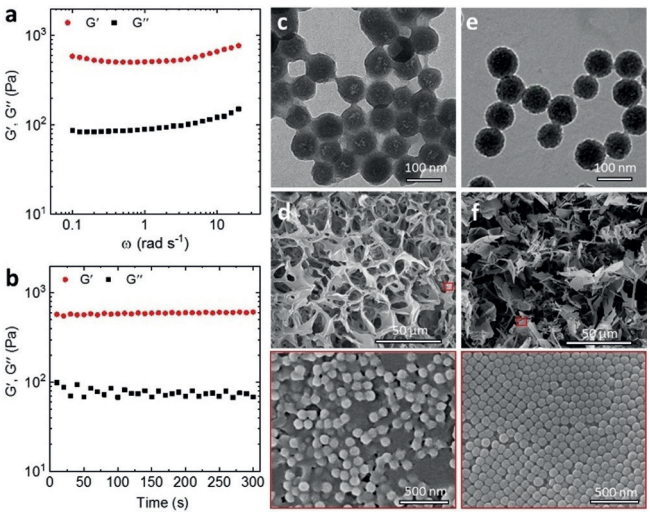

Figure 2. Rheological and morphological characterization of the DNA-SiNP nanocomposite hydrogel. a) Frequency sweep test between 0.1 and 20 rad s^{-1} at a fixed strain of 1%. b) Time-scan rheological test performed with a fixed strain of 1% and a fixed frequency (1 Hz) for 5 min. The data in (a) and (b) were collected by rotational rheometry at 25 °C. Representative c, e) TEM and d, f) SEM images at different magnifications. The lower two panels of the SEM images shown in (d) and (f) are magnifications of the red framed regions in the corresponding upper two panels. The samples were obtained from **SiNP-Ih** (c, d) or, as a control, **SiNP-Ic** (e, f) subjected to the C-HCR polymerization.

assembly of the hairpin strands **h1**, **h2** and **H1**, **H2** to initiate gelation of the DNA-SiNP composite material (Figure 1).

The C-HCR strategy depicted in Figure 1 was adopted from the original work, wherein the C-HCR method was established for the production of pure DNA hydrogels.[12] In our work described here, the two-step amplification procedure was implemented to ensure efficient linkage and homogeneous integration of the DNA-SiNPs with the DNA hydrogel. In a first step, covalently linked **SiNP-Ih** and hairpin strands **h1**, **h2** were allowed to react to form linear chains on the SiNP from which a single-stranded b′-c segment protrudes (Figure 1). This reaction was carried out for 12 h, and the resulting particles were purified by centrifugation and then allowed to react with the hairpin strands **H1** and **H2**-dimer. In this second step, **H1** and **H2**-dimer hybridized with the particle-bound b′-c segments to initiate the formation of clamped 3D networks by C-HCR (Figures 1; for a detailed description and analysis of the C-HCR, see Figures S2 and S3).

Dynamic light scattering (DLS) analysis of the C-HCR process with **SiNP-Ih** prepolymerized by **h1**/**h2**-mediated linear HCR clearly indicated that polymeric composites were formed within 72 h, whereas control experiments with **SiNP-Ic** containing a random ssDNA sequence (Table S1) showed no increase in the hydrodynamic diameter, thus excluding the possibility of unspecific aggregation (Figure S4). Rotational rheology was used to study the bulk mechanical properties of the DNA-SiNP nanocomposite hydrogels (Figure 2a, b and Figure S5). We observed a significant degree of elasticity, with the storage modulus G′ always being larger than the loss modulus G″, and extracted a constant elastic modulus of $G_0 \approx 550$ Pa. Furthermore, both the storage modulus G′ and the loss modulus G″ are rather invariable during time-scan tests, indicating the mechanical stability of the nanocomposite hydrogel under the rotational measurements (Figure 2b). Importantly, the G_0 value of the pure DNA hydrogel lacking SiNPs was determined as approximately 280 Pa (Figure S6), which is about twofold lower than that of the DNA-SiNP nanocomposite materials. We attribute the larger constant elastic modulus to the reinforcement of the polymerized DNA scaffold by the incorporated SiNPs.

The structural features of the novel DNA-SiNP hydrogels were analyzed by transmission electron microscopy (TEM) and scanning electron microscopy (SEM). The TEM images clearly indicated the presence of DNA, which coated the **SiNP-Ih** and served as a crosslinker between the particles (Figure 2c), which is in agreement with the design of the C-HCR process (Figure S3). As a consequence, the DNA-SiNP nanocomposite materials possess an amorphous morphology and a distinctive hierarchical ultrastructure, as indicated by SEM analysis (Figure 2d). In contrast, control samples prepared with non-complementary **SiNP-Ic** showed discrete particles as well as particle superlattices that were formed by aggregation in the course of dehydration during specimen preparation (Figure 2e, f). Thus, these results show that the targeted binding of the DNA oligomers is essential to achieve a homogeneous distribution of the nanoparticles in the polymer hydrogels.

We then investigated whether the self-assembly of DNA-SiNP nanocomposite materials is possible at the interface of microfluidically produced water-in-oil (W/O) droplets (Figure 3). To this end, a microfluidic flow-focusing T-junction droplet generator chip, fabricated by micromilling as previously reported,[13] was used to disperse an aqueous solution of the C-HCR mixture in a continuous oil phase (Figure 3a). Specifically, the oil phase contained the positively charged 1,2-dioleoyl-3-trimethylammoniumpropane (DOTAP) lipid to generate a positively charged inner surface

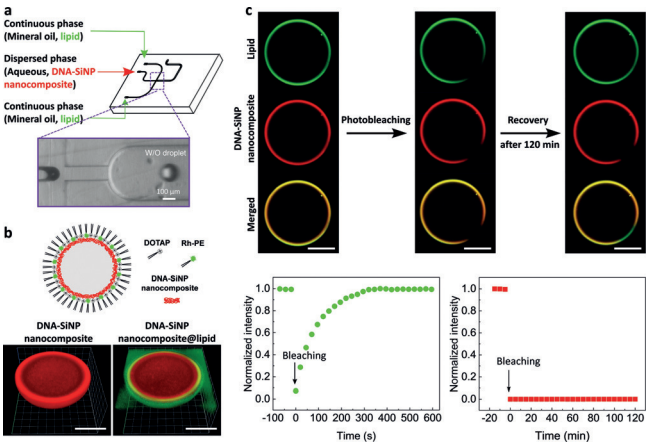

Figure 3. Self-assembly of DNA-SiNP nanocomposite hollow microspheres inside W/O droplets. a) Schematic illustration of the microfluidic droplet generator chip and high-speed camera image of a formed W/O droplet. b) Schematic illustration of the W/O droplet (top) with a positively charged DOTAP lipid shell (green) as the outer membrane and the negatively charged DNA-SiNP nanocomposite as the inner shell (red). Note that the high-resolution 3D images at the bottom clearly indicate the double-layer structure of the self-assembled spherical constructs. c) FRAP analysis of the hollow-sphere constructs. The images show W/O droplets before and after photobleaching. A time-course analysis of the fluorescence recovery after photobleaching is shown in the graphs below. All scale bars in (b) and (c) are 50 µm.

in the W/O droplets (see the schematic illustration in Figure 3b and Figure S7). The dispersed aqueous phase contained **SiNP-Ih** particles that were prepolymerized by **h1**/**h2**-mediated linear HCR, as described above, in addition to the **H1** and **H2** hairpin strands. To enable visualization of the droplets by fluorescence microscopy, the DOTAP was doped with 1,2-dimyristoyl-*sn*-glycero-3-phosphoethanolamine-*N*-(lissamine rhodamine B sulfonyl) (Rh-PE) lipid (0.1 mol%, green in Figure 3), and the SiNPs were labeled with the fluorescent dye Cy5 (red in Figure 3) by a previously reported method.[11d]

Using the microfluidic droplet generator, stable W/O droplets (ca. 120 µm diameter) were produced and collected for analysis by means of confocal fluorescence microscopy (Figures 3b,c; see also Figure 4a). The images clearly showed that the DNA-SiNP nanocomposite materials formed hollow

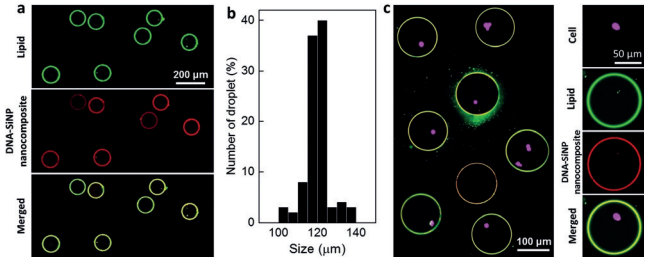

Figure 4. Production of DNA-SiNP nanocomposite hollow spheres and use as cell containers. a) Fluorescence images and b) size distribution of collected DNA-SiNP nanocomposite hollow spheres. c) Addition of CHO-S cells to the dispersed phase led to formation of cell-loaded nanocomposite containers (see also Figure S11). All images show the lipid membrane, SiNPs, and cells in green, red, and violet, respectively.

microspheres that spontaneously accumulated underneath the DOTAP membrane, and the droplets indeed exhibited the expected double-layered interface morphology (Figure 3b). High-resolution imaging indicated that the DNA-SiNP composite shell had a homogeneous thickness of 4–6 µm. Importantly, no such layered structures were observed in control experiments, where zwitterionic POPC (1-palmitoyl-2-oleoyl-*sn*-glycero-3-phosphocholine) was used instead of the positively charged DOTAP (Figures S7 and S8). Therefore, the results conclusively supported the hypothesis that electrostatic interactions between the positively charged lipid membrane and the negatively charged DNA-SiNP composite led to formation of the proposed double-layered hollow microsphere structure.

To shed light on the phase segregation and layer formation, the spontaneous assembly of DNA-SiNP nanocomposites underneath the positively charged lipid membrane was also studied by real-time fluorescence imaging (Figure S9). The results indicated that a mixture of prepolymerized **SiNP-Ih** and **H1**/**H2** hairpins allocate underneath the positively charged lipid membrane significantly faster than **SiNP-Ih** only. This observation is consistent with the hypothesis that the increased negative charge caused by the polymerization of the composite materials accelerates the electrostatic phase separation of the components in the W/O droplets. Furthermore, the polymeric nature of the DNA-SiNP nanocomposite shell was confirmed by fluorescence recovery after photobleaching (FRAP) experiments (Figure 3c). The data clearly showed that no diffusion of the embedded SiNPs (red) occurred, whereas fluorescence recovery of the lipids indicated the high fluidity of the lipid shell (green). Control experiments performed with **SiNP-Ic** under the same conditions showed a similar fluorescence recovery rate of the lipid envelope to that observed in Figure 3c (ca. 5 min). However, the **SiNP-Ic** also diffused back into the bleached area within this time period (ca. 6 min; see Figure S10). Thus, the results clearly show that the composite materials can indeed be assembled into supramolecular, microstructured hollow-sphere architectures.

As the microfluidic droplet generator generated the W/O droplets with a frequency of approximately 20 Hz, the microstructured hollow spheres could be produced with a high throughput. Statistical analysis of the spheres showed a high homogeneity in the size distribution with a distinct maximum at about 120 µm (Figure 4a,b). With regard to possible applications, we wanted to examine whether such hollow spheres could in principle be used as containers for the encapsulation of cells. To investigate whether supramolecular self-assembly of the nanocomposites also works in complex media and in the presence of enclosed cells, cell culture medium containing CHO-S cells was supplemented with the C-HCR components and used as the dispersed phase. The concentration of the cells was adjusted so that statistically, about 80% of the droplets contained cells (Figure S11a). In fact, fluorescence microscopy analysis clearly revealed the formation of cell-loaded hollow spheres (Figure 4c and Figure S11). These preliminary experiments thus show that the synthesis strategy presented herein has potential for applications in the life sciences.

In summary, we have shown that by applying the two-step clamped hybridization chain reaction to the surface of nanoparticles, novel composite materials can be produced from silica nanoparticles and DNA polymers. These materials can be assembled in bulk as well as in thin layers within microfluidically generated water-in-oil droplets. The latter approach enables mechanically stabilized hollow spheres with uniform size distributions to be produced at high throughput rates. We believe that this concept represents an important contribution to the further development of bottom-up fabrication methods as the supramolecular self-assembly of DNA materials can be further refined by appropriate sequence design, for example, to include non-nucleic acid components in such architectures. In addition, this approach could be used for applications in the life sciences, for example, to develop compartmentalized reaction systems for biocatalytic applications or arrangements of cell containers for cell biology studies.[14]

Acknowledgements

We acknowledge funding from the Helmholtz programme "BioInterfaces in Technology and Medicine". This project was supported by the KIT research initiative "VirtMat" and through GRK 2039 funded by the German Research Foundation (DFG). Y.H. is grateful for a Ph.D. fellowship from the China Scholarship Council (CSC). We also thank Volker Zibat (LEM, KIT) for electron microscopy.

Conflict of interest

The authors declare that a patent application for DNA-SiNP composite materials has been filed.

Keywords: DNA hybridization chain reaction · DNA nanotechnology · hollow microspheres · microfluidics · nanomaterials

How to cite: *Angew. Chem. Int. Ed.* **2019**, *58*, 17269–17272
Angew. Chem. **2019**, *131*, 17429–17432

[1] M. R. Jones, N. C. Seeman, C. A. Mirkin, *Science* **2015**, *347*, 1260901.

[2] a) N. C. Seeman, *Nature* **2003**, *421*, 427–431; b) D. Yang, M. R. Hartman, T. L. Derrien, S. Hamada, D. An, K. G. Yancey, R. Cheng, M. Ma, D. Luo, *Acc. Chem. Res.* **2014**, *47*, 1902–1911; c) F. Hong, F. Zhang, Y. Liu, H. Yan, *Chem. Rev.* **2017**, *117*, 12584–12640; d) Q. Hu, H. Li, L. Wang, H. Gu, C. Fan, *Chem. Rev.* **2019**, *119*, 6459–6506; e) M. Madsen, K. V. Gothelf, *Chem. Rev.* **2019**, *119*, 6384–6458; f) F. C. Simmel, B. Yurke, H. R. Singh, *Chem. Rev.* **2019**, *119*, 6326–6369; g) Y. Hu, C. M. Niemeyer, *Adv. Mater.* **2019**, *31*, 1806294.

[3] W. M. Shih, C. Lin, *Curr. Opin. Struct. Biol.* **2010**, *20*, 276–282.

[4] C. M. Niemeyer, *Angew. Chem. Int. Ed.* **2010**, *49*, 1200–1216; *Angew. Chem.* **2010**, *122*, 1220–1238.

[5] D. A. Giljohann, D. S. Seferos, W. L. Daniel, M. D. Massich, P. C. Patel, C. A. Mirkin, *Angew. Chem. Int. Ed.* **2010**, *49*, 3280–3294; *Angew. Chem.* **2010**, *122*, 3352–3366.

[6] J. Li, L. Mo, C.-H. Lu, T. Fu, H.-H. Yang, W. Tan, *Chem. Soc. Rev.* **2016**, *45*, 1410–1431.

[7] A.-K. Schneider, C. M. Niemeyer, *Angew. Chem. Int. Ed.* **2018**, *57*, 16959–16967; *Angew. Chem.* **2018**, *130*, 17204–17212.

[8] a) H. Song, D. L. Chen, R. F. Ismagilov, *Angew. Chem. Int. Ed.* **2006**, *45*, 7336–7356; *Angew. Chem.* **2006**, *118*, 7494–7516; b) S. Sevim, A. Sorrenti, C. Franco, S. Furukawa, S. Pané, A. J. deMello, J. Puigmartí-Luis, *Chem. Soc. Rev.* **2018**, *47*, 3788–3803.

[9] a) I. Platzman, J.-W. Janiesch, J. P. Spatz, *J. Am. Chem. Soc.* **2013**, *135*, 3339–3342; b) M. Weiss, J. P. Frohnmayer, L. T. Benk, B. Haller, J.-W. Janiesch, T. Heitkamp, M. Börsch, R. B. Lira, R. Dimova, R. Lipowsky, E. Bodenschatz, J.-C. Baret, T. Vidakovic-Koch, K. Sundmacher, I. Platzman, J. P. Spatz, *Nat. Mater.* **2017**, *17*, 89; c) K. Jahnke, M. Weiss, C. Frey, S. Antona, J.-W. Janiesch, I. Platzman, K. Göpfrich, J. P. Spatz, *Adv. Funct. Mater.* **2019**, *29*, 1808647.

[10] C. Kurokawa, K. Fujiwara, M. Morita, I. Kawamata, Y. Kawagishi, A. Sakai, Y. Murayama, S.-i. M. Nomura, S. Murata, M. Takinoue, M. Yanagisawa, *Proc. Natl. Acad. Sci. USA* **2017**, *114*, 7228–7233.

[11] a) L. R. Hilliard, X. Zhao, W. Tan, *Anal. Chim. Acta* **2002**, *470*, 51–56; b) P. P. Pillai, S. Reisewitz, H. Schroder, C. M. Niemeyer, *Small* **2010**, *6*, 2130–2134; c) X. D. Wang, K. S. Rabe, I. Ahmed, C. M. Niemeyer, *Adv. Mater.* **2015**, *27*, 7945–7950; d) A. Leidner, S. Weigel, J. Bauer, J. Reiber, A. Angelin, M. Grösche, T. Scharnweber, C. M. Niemeyer, *Adv. Funct. Mater.* **2018**, *28*, 1707572; e) A. Leidner, J. Bauer, M. Ebrahimi-Khonachah, M. Takamiya, U. Strähle, T. Dickmeis, K. S. Rabe, C. M. Niemeyer, *Biomaterials* **2019**, *190–191*, 76–85; f) P. Sun, A. Leidner, S. Weigel, P. G. Weidler, S. Heissler, T. Scharnweber, C. M. Niemeyer, *Small* **2019**, *15*, 1900083.

[12] J. Wang, J. Chao, H. Liu, S. Su, L. Wang, W. Huang, I. Willner, C. Fan, *Angew. Chem. Int. Ed.* **2017**, *56*, 2171–2175; *Angew. Chem.* **2017**, *129*, 2203–2207.

[13] M. Grösche, A. E. Zoheir, J. Stegmaier, R. Mikut, D. Mager, J. G. Korvink, K. S. Rabe, C. M. Niemeyer, *Small* **2019**, *15*, 1901956.

[14] Cell-loaded microcontainers have been used, for instance, for miRNA detection on the single-cell level (S. Guo, W. N. Lin, Y. Hu, G. Sun, D.-T. Phan, C.-H. Chen, *Lab Chip* **2018**, *18*, 1914–1920) or functional cell screening (A. I. Segaliny, G. Li, L. Kong, C. Ren, X. Chen, J. K. Wang, D. Baltimore, G. Wu, W. Zhao, *Lab Chip* **2018**, *18*, 3733–3749). In view of the outstanding attractiveness of DNA-silica materials for cell adhesion (see Ref. [11d,f]), we believe that the hollow-sphere containers presented here could also be applicable for high-throughput cell adhesion studies.

Manuscript received: August 20, 2019
Version of record online: October 18, 2019

